

Understanding the resistivity and absolute thermoelectric power of disordered metals and alloys

This article has been downloaded from IOPscience. Please scroll down to see the full text article.

2008 J. Phys.: Condens. Matter 20 114103

(<http://iopscience.iop.org/0953-8984/20/11/114103>)

View [the table of contents for this issue](#), or go to the [journal homepage](#) for more

Download details:

IP Address: 129.252.86.83

The article was downloaded on 29/05/2010 at 11:07

Please note that [terms and conditions apply](#).

Understanding the resistivity and absolute thermoelectric power of disordered metals and alloys

Jean-Georges Gasser

Laboratoire de Physique des Milieux Denses, Institut de Chimie, Physique et Matériaux,
Université Paul Verlaine-Metz, 1 Bd Arago, 57078 Metz cedex 3, France

E-mail: gasser@univ-metz.fr

Received 30 August 2007

Published 20 February 2008

Online at stacks.iop.org/JPhysCM/20/114103

Abstract

We recall definitions of the electronic transport properties, direct coefficients like electrical and thermal transport conductivities and crossed thermoelectric coefficients like the Seebeck, Peltier and Thomson coefficients. We discuss the links between the different electronic transport coefficients and the experimental problems in measuring these properties in liquid metals.

The electronic transport properties are interpreted in terms of the scattering of electrons by 'pseudo-atoms'. The absolute thermoelectric power (ATP), thermopower or Seebeck coefficient is known as the derivative of the electrical resistivity versus energy. The key is to understand the concept of resistivity versus energy.

We show that the resistivity follows approximately a $1/E$ curve. The structure factor modulates this curve and, for a Fermi energy corresponding to noble and divalent metals, induces a positive thermopower when the free electron theory predicts a negative one. A second modulation is introduced by the pseudopotential squared form factor or equivalently by the squared t matrix of the scattering potential. This term sometimes introduces an anti-resonance (divalent metals) which lowers the resistivity, and sometimes a resonance having an important effect on the transition metals. Following the position of the Fermi energy, the thermopower can be positive or negative. For heavy semi-metals, the density of states splits into an s and a p band, themselves different from a free electron $E^{0.5}$ curve. The electrons available to be scattered enter the Ziman formula. Thus if the density of states is not a free electron one, a third modulation of the $\rho \cong 1/E$ curve is needed, which also can change the sign of the thermopower.

For alloys, different contributions weighted by the concentrations are needed to explain the concentration dependent resistivity or thermopower. The formalism is the same for amorphous metals. It is possible that this mechanism can be extended to high-temperature crystalline alloys or even disordered semiconductors since we can separate the transport coefficients between the effect of the number of charge carriers and a scattering term linked to carrier mobility.

(Some figures in this article are in colour only in the electronic version)

1. Introduction

The subject of this work is mainly the understanding of the trends of the thermopower of liquid and amorphous metals (normal, noble, transition, semi-metals and alloys) as a function of valence, composition, temperature, pressure, ... linked to the behaviour of the electrical resistivity. It is not excluded that the developed formalism may be adapted

to explain these properties in the case of solid alloys or compounds.

2. The electronic transport coefficients

If the electrical and thermal conductivity are in general well understood, this is not the case for the thermoelectric effects (Peltier, Thomson and Seebeck), which are more complex.

The electronic transport coefficients and the equations between them are well described in the book *Electronic Conduction in Solids* by Smith, Janak and Adler [1]. The specific case of metals and metallic alloys is described in Barnard's [2] book *Thermoelectricity in Metals and Alloys*. The terminology used below is that used by these authors.

In general a gradient of something induces a force, which itself induces a density of flux. The problem is to make a proper choice of fluxes and forces [1]. A gradient of potential $\vec{\nabla}V$ induces a density of electric current \vec{J} . The electrical conductivity σ is defined by the relation $\vec{J} = -\sigma\vec{\nabla}V$ when $\vec{\nabla}T = 0$. A gradient of temperature $\vec{\nabla}T$ induces a density of heat flux \vec{Q} . The thermal conductivity λ is defined by the relation $\vec{Q} = -\lambda\vec{\nabla}T$ when $\vec{J} = 0$. But a gradient of temperature can also induce an electric current and a gradient of potential can induce a heat flux. These phenomena are called the thermoelectric effects.

The current density and the heat flux density are linked to gradients of temperature and potential respectively [1, 3] by

$$\begin{aligned}\vec{J}_e &= e^2 K_{11} \vec{E} - (e/T_K) K_{12} (-\vec{\nabla}T_K) \\ \vec{Q}_e &= -\|e\| K_{21} \vec{E} + (1/T_K) K_{22} (-\vec{\nabla}T_K),\end{aligned}\quad (1)$$

where \vec{J}_e is the density of current, \vec{Q}_e is the density of heat flux and $-\vec{E} = \vec{\nabla}V$ is the gradient of potential

The coefficients K_{ij} are not directly measured or experimentally measurable. It is necessary to introduce other (more) physical quantities.

At zero temperature gradient (uniform temperature) we have

$$\vec{J}_e = \sigma \vec{E} = -\sigma \vec{\nabla}V \quad (2)$$

$$\sigma = e^2 K_{11}. \quad (3)$$

This is the so-called microscopic Ohm law; σ is the electrical conductivity.

Always at zero temperature gradient we have

$$\vec{Q} = -\|e\| K_{21} \vec{E} = -\frac{\|e\| K_{21}}{e^2 K_{11}} \vec{J}_e = \pi \vec{J}_e, \quad (4)$$

π being the Peltier coefficient of a component (pure metal or alloy).

At zero density of current $\vec{J}_e = 0$ (one opens the circuit)

$$\vec{Q}_e = -\lambda \vec{\nabla}T, \quad (5)$$

with $\lambda = \frac{K_{22} K_{11} - K_{12} K_{21}}{T_K K_{11}}$ this is the Fourier law: λ is the thermal conductivity.

Always at zero density of current we have

$$\vec{E} = \frac{-K_{12}}{(\|e\| K_{11} T_K)} (-\vec{\nabla}T_K) = S \vec{\nabla}T_K. \quad (6)$$

S is the absolute thermoelectric power (or Seebeck coefficient) of a component (pure or alloy). A relation between π and S can be found:

$$\pi = \frac{-K_{21}}{K_{12}} T_K S = T_K S. \quad (7)$$

This is the first Kelvin relation. The second Kelvin (–Onsager) relation links the Thomson coefficient h to the Seebeck coefficient S (see Barnard [2], equation 1.73):

$$h = T_K \frac{dS}{dT_K}. \quad (8)$$

Thus the knowledge of one of the Peltier, Thomson and Seebeck effects induces the knowledge of the two others, either by an algebraic relation (first Kelvin's law) or by an integration or derivation (second Kelvin's law).

The electric current carried by one electron is $e\vec{v}f_k$. The heat flux carried by one electron is $(E_k - \mu_e)\vec{v}f_k$. The current and the heat carried by all the electrons in conductors are

$$\vec{J} = q \int_{ZB} \vec{v} f_k \frac{dV_k}{4\pi^3} \quad (9)$$

and

$$\vec{Q} = q \int_{ZB} (E_k - \mu_e) \vec{v} f_k \frac{dV_k}{4\pi^3}. \quad (10)$$

If the calculation is carried out, one can finally show that for metals one has (Barnard [3], equation 3.57)

$$S(E) = \frac{\pi^2 k_B^2 T_K}{3e} \left[\frac{\partial \ln \sigma(E)}{\partial E} \right]_{E=\mu_F} \quad \text{or} \quad (11)$$

$$S(E) = \frac{\pi^2 k_B^2 T_K}{3|e|E} \left| \frac{\partial \ln(\rho(E))}{\partial \ln(E)} \right|$$

and

$$\lambda = \frac{(L_0 - S^2) T_K}{\rho} \cong \frac{L_0 T_K}{\rho}. \quad (12)$$

The approximation of equation (12) which neglects the thermopower S is known as the Wiedemann–Franz law with $L_0 = \frac{\pi^2 k_B^2}{3e^2} L_0$ where L_0 is the ‘Sommerfeld value of the Lorenz number’. There is however no problem in using the exact expression of equation (12) if the thermopower is measured.

To summarize: a potential gradient creates a density of current. At zero temperature gradient, it defines σ . A temperature gradient creates a density of heat flux. At zero density of current it defines λ . Crossed effects exist: a temperature gradient creates an electric field (Seebeck effect) and a density of current creates a density of heat flux (Peltier effect). The three thermoelectric effects (Peltier, Seebeck and Thomson) are linked by the two Kelvin's laws. The Seebeck coefficient is proportional to the derivative of the electrical resistivity with respect to the (Fermi) energy. The thermal conductivity is linked to the electrical conductivity and to the Seebeck coefficient. A simplified expression where the thermopower S is neglected is called the Wiedemann–Franz law. It has been shown [4] that for liquid metals this law is valid with an accuracy of 1–10% (see figure 4 of [4]). Thus measuring two properties allows the knowledge of all the electronic transport properties which are very sensitive to the chemical ordering. This is important because it is easier to measure accurately the electrical conductivity and the thermopower than the thermal conductivity. Indeed, λ is supposed to be measured in a static fluid. This never

occurs because the gradient of temperature, which is necessary to measure λ , also creates convective effects (except in microgravity!). Moreover, the Seebeck coefficient can be related to the electrical conductivity by a derivation with regard to energy of the electrical resistivity [2].

3. Thermoelectric coefficients measured in the laboratory

One cannot practically measure the Seebeck and Peltier coefficients of a single component (pure element or alloy), using equations (4) and (6). From an experimental point of view one can only measure the difference of two ‘absolute thermoelectric powers’ of two components by realizing a ‘(thermo-) couple’. To get the ‘absolute’ thermopower of a component it is necessary to measure the e.m.f. of a couple, to differentiate it with respect to temperature and to subtract the ‘absolute’ thermopower of the second component constituting the couple. Thus it is necessary to know the absolute thermoelectric power of at least one component.

The Thomson coefficient of a component (metal or alloy) is the only ‘absolute’ coefficient of a component which is directly measurable (it does not need a junction but it is a very difficult experiment). If a current passes through a wire where a temperature gradient exists, a release or absorption of heat exists, following the direction of the current and of the temperature gradient, and proportional to the Thomson coefficient. Practically, this has been done at the National Bureau of Standards by Roberts [5] for very pure platinum (called ‘platinum 67’).

Using the second Kelvin law $S(T) = \int_{T=0}^T \kappa \frac{h dT}{T^2}$ one can deduce the Seebeck coefficient of an element by integrating the Thomson coefficient from zero kelvin to the considered temperature. It needed three different very accurate calorimeters (the reversible Thomson effect is about a hundred times smaller than the quadratic Joule effect) and thanks to Roberts [5] ‘platinum 67’ is now the standard of thermoelectricity.

Knowing the ATP of one component and measuring the ATP of a couple, we can obtain the ATP of all components. In our laboratory we calibrate systematically all wires that we use for thermoelectric measurements in general pure tungsten and tungsten–26% rhenium which are not dissolved in liquid metals. Our most used experimental cell is represented in figure 1. A gradient of temperature or of potential may be applied to the liquid (or solidified) sample.

4. Understanding the physics of the electronic transport properties of liquid metals and alloys

In dense matter, the internal electrons are scattered by the ions in the presence of the other electrons. These internal electrons behave as neutrons or x-rays scattered by dense matter and the formalism is similar for pure metals and alloys.

The electrical resistivity ρ and the thermoelectric power S can be calculated by using the Ziman formula [6] for pure

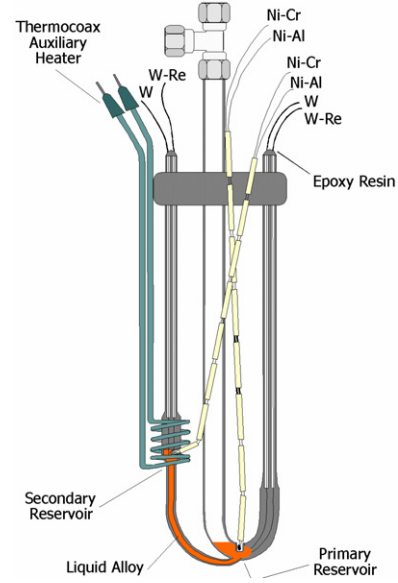


Figure 1. Resistivity and thermopower measurement cell. The measurement of the resistivity needs a long capillary and four electrodes. The measurement of the ATP needs a gradient of temperature and two couples immersed in the liquid metal (or in electrical contact with it).

metals or the Faber–Ziman one [7] for alloys. The resistivity of a pure metal is given by the formula

$$\rho = \frac{3\pi^2 m^2 \Omega_0}{e^2 \hbar^3 k_F^2} \int_0^1 a(q) v^2(q) 4 \left(\frac{q}{2k_F} \right)^3 d \left(\frac{q}{2k_F} \right). \quad (13)$$

$a(q)$ is the structure factor, $v(q)$ the model pseudopotential form factor, k_F the Fermi wavevector, Ω_0 the mean atomic volume and q the scattering wavevector (the other symbols have their usual meanings). For liquid alloys, the term $a(q) v^2(q)$ is simply replaced by

$$c_1 v_1^2 [1 - c_1 + c_1 a_{11}(q)] + c_2 v_2^2 [1 - c_2 + c_2 a_{22}(q)] + 2c_1 c_2 v_1 v_2 [a_{12}(q) - 1]. \quad (14)$$

The a_{ij} ($i, j = 1$ or 2 for a binary alloy) are the set of partial structure factors, the c_i are the concentrations and the v_i are the model potential form factors *in the alloy*.

This formalism, valid only for normal metals, was first extended to noble, transition, rare earth and semi-metals by Evans [8] and to alloys by Dreirach *et al* [9] and others. Thus the formalism is now general. The pseudopotential form factor has been replaced by a t matrix expressed in terms of phase shifts η_l of an incident plane wave scattered by a spherically symmetrical potential. This method, called the ‘method of the neutral pseudo-atoms’, consists of starting with the potential of an atom corrected by taking into account exchange and correlation as described by Makradi *et al* [10]. To this potential correspond the term energies of the electrons on the different electronic levels (figure 2). In dense matter, neighbouring atoms lead to a superposition of their potentials. There is no longer an asymptotic value of the potential tending to the zero energy relative to vacuum (electron at infinity with zero velocity), the highest potential is negative and the external

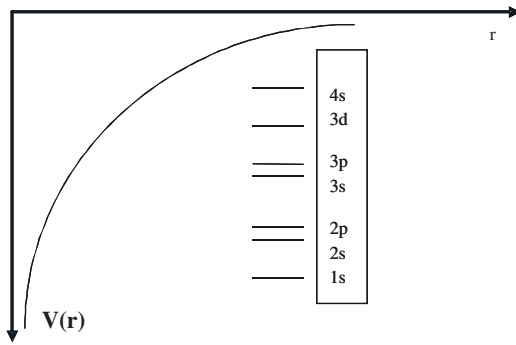


Figure 2. Schematic pseudo-neutral atom potential.

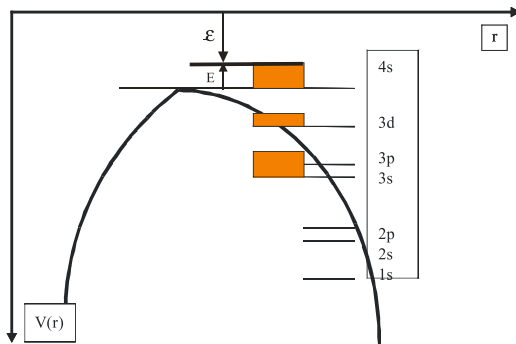


Figure 3. Schematic potential for dense matter and apparition of bands.

electrons of the atom give rise to energy bands (figure 3). Two energies have been used: the energy ϵ relative to vacuum used in the model pseudopotential formalism and the energy E relative to the highest value of the potential barrier (in the muffin tin approximation that we presently use).

4.1. Effect of temperature and pressure

In this representation (figure 4) the effect of temperature and pressure can be well understood. The pressure tends to decrease the interatomic distance while the temperature tends to increase it. If there are practically no limits to increasing pressure, increasing temperature reaches its limit rapidly because of a liquid–vapour transformation. To keep the fluid in its liquid form, it is necessary also to increase pressure, but temperature remains the dominant effect. We speak about expanded liquid metals. It is clear on figure 4 that the Fermi energy E relative to the highest potential value decreases with temperature and can even become negative, that leads to a localization of the electrons and explains the metal–non-metal transition. Inversely, high pressures increase the metallic behaviour.

4.2. Muffin potentials, density of states and Fermi energy

Practically, if one has to make calculations, we need in dense matter a spherical potential. Thus we use the muffin tin approximation as described by Dreirach *et al* [9]. For r values between zero and the muffin tin radius R_{MT} the

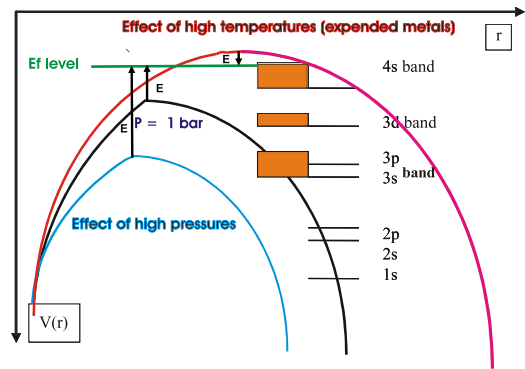


Figure 4. Effect of pressure and temperature on the Fermi energy of liquid metals.

potential is the result of the superposition of neighbouring atoms weighted by their probability to be at a given distance according to the Mukhopadhyay *et al* [11] method. To take the interstitial region into account, a constant overlapping potential is constructed between the muffin tin radius R_{MT} and the Wigner–Seitz radius R_{WS} . We have represented in figure 5 the muffin tin potential on the same scale as the electron energies, i.e. the density of states, inverting the commonly used axes. The energies used have to be clarified. We use the symbol ϵ if we refer to the energy of vacuum. On this scale the muffin tin potential zero ϵ_{MTZ} relative to an absolute energy scale is represented. The energy E of electrons in the conduction band is pertinently taken relative to the muffin tin zero potential as well as the Fermi energy E_F . The different approximations used are represented in figure 5. Dreirach *et al* [9] considered a free electron band whose bottom is at E_B (positive or negative) from the muffin tin zero potential. The energy relative to the muffin tin zero potential is $E = E_B + \frac{\hbar^2 k^2}{2m^*}$; respectively, the Fermi energy is

$$E_F = E_B + \frac{\hbar^2 k_F^2}{2m^*}. \quad (16)$$

Esposito *et al* [12] considered that $E_B = 0$ but correct the free electron density of states (in fact the integrated density of states) by a contribution due to Lloyd [13] which is an explicit function of the scattering phase shifts at energy E . This method corrects the density of states and allows the description of noble and transition metals. In our approach, considering that the density of states has to be corrected and that there is no reason why the bottom of the band is exactly at the level of the muffin tin zero potential, we combined both approaches. Moreover, taking into account that some heavy polyvalent metals like lead or bismuth may split their sp electrons into two bands, we took this into account (Ben Abdellah *et al* [14]). In Esposito’s [12] approach the Fermi energy is calculated differently since the formula between E , E_B and k is no longer valid. The Fermi energy is determined by filling the density of states by Z (an integer) electrons. Then we deduce k_F by

$$k_F = \frac{(2mE_F)^{1/2}}{\hbar} \quad (17)$$

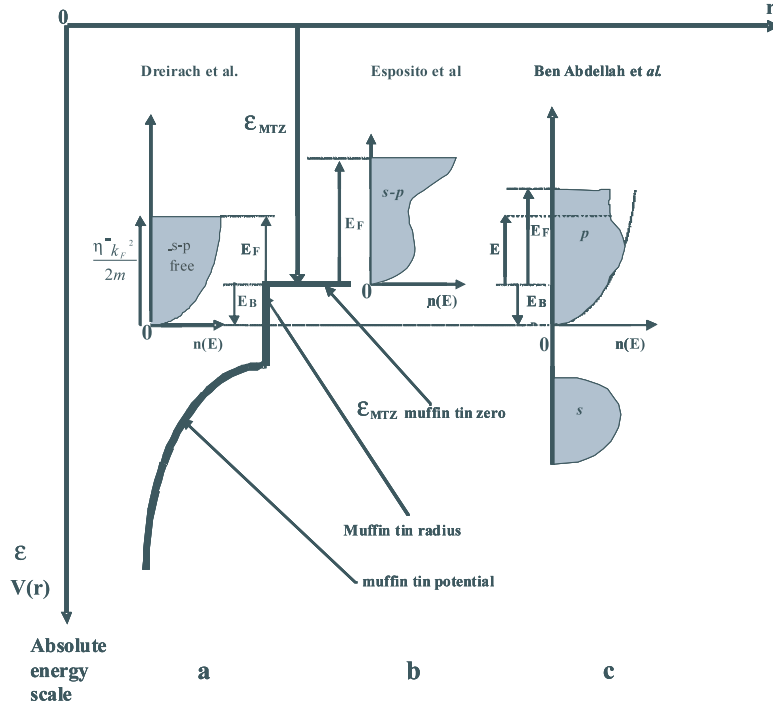


Figure 5. Comparison of the muffin tin potential with different shapes and positions of the conduction band.

and obtain an effective valence N_C (not necessarily an integer) from k_F by

$$N_C = \frac{k_F^3 \Omega_0}{3\pi^2}, \quad (18)$$

where Ω_0 is the atomic volume.

4.3. Energy dependent resistivity and thermopower

The extended Ziman formula can be written in an energy dependent form:

$$\rho(E) = \frac{3\pi^2 m_e^2 \Omega_0}{4e^2 \hbar^3 k^6} \int_0^{2k} a(q) |t(q, E)|^2 q^3 dq, \quad (19)$$

where Ω_0 is the atomic volume and $a(q)$ is the structure factor. The squared t matrix $|t(q, E)|^2$ replaces the squared form factor of equation (13) and is characteristic of the scattering of an electron by a muffin tin potential for the electron having the energy E above the muffin tin zero potential, q is the wavevector transfer between the incident electron wave and the scattered electron wave, E is linked to k by

$$E = \hbar^2 k^2 / (2m^*) + E_B \quad (20)$$

and the t matrix is

$$t(q, E) = -\frac{2\pi \hbar^3}{m \sqrt{2mE} \Omega_0} \times \sum_{\ell} (2\ell + 1) \sin \eta_{\ell}(E) \exp(i\eta_{\ell}(E)) P_{\ell}(\cos \theta). \quad (21)$$

In the extended Ziman formula (formula (19)), the energy appears in the prefactor ($1/k^6$), in the upper integral limit k and in the t matrix $t(q, E)$. If one wants to compare to an experimental resistivity, the energy E has to be taken at E_F and the wavevector k at k_F .

4.3.1. Normal metals. The thermopower (or absolute thermoelectric power (ATP) or Seebeck coefficient) is the derivative of the resistivity (formula (11)); it is thus important to know the shape of the resistivity versus energy curve. In a first crude approximation we can consider that the product $a(q)t(q)^2$ is approximately a constant. The Ziman formula can then be integrated analytically and gives a resistivity proportional to $1/E$ (figure 6). This is consistent with figure 4. Indeed, application of pressure increases the distance between the highest value of the potential and the Fermi energy, thus metallizes the system more. Conversely, increasing the temperature, thus the distance between atoms, leads to a metal–non-metal transition. The system becomes insulating when the Fermi energy becomes lower than the potential barrier, i.e. when energy $E \leq 0$. The resistivity being a decreasing function of energy, the ATP of liquid metals is theoretically always negative. In figure 7(a) [10] we plotted the resistivity of liquid germanium as a function of energy with several *ab initio* calculations. The resistivity is effectively a decreasing function of energy, thus the ATP (figure 7(b)) is negative as observed experimentally. This rule explains the negative thermopower for most of the polyvalent liquid metals (In, Ga, Al, Ge, Sn, Pb, Bi).

4.3.2. Noble and divalent metals. However, some metals do not obey this rule. This is the case for some divalent metals like zinc and for noble metals like copper and silver. The positive sign is in contradiction with our first crude approximation $a(q)|t(q)|^2 \approx \text{constant}$. But an explanation can easily be found. One must only remember that the structure factor is a curve which presents a sharp maximum, thus it is necessary to modulate the $1/E$ resistivity curve by the maximum of the

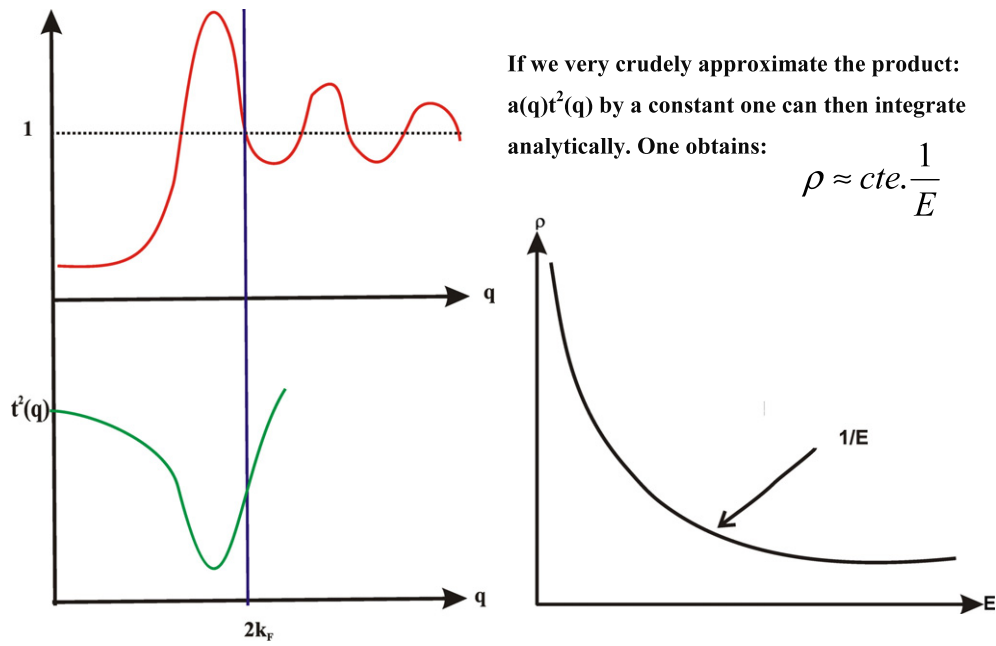


Figure 6. Why the resistivity versus energy is nearly 1/E-like.

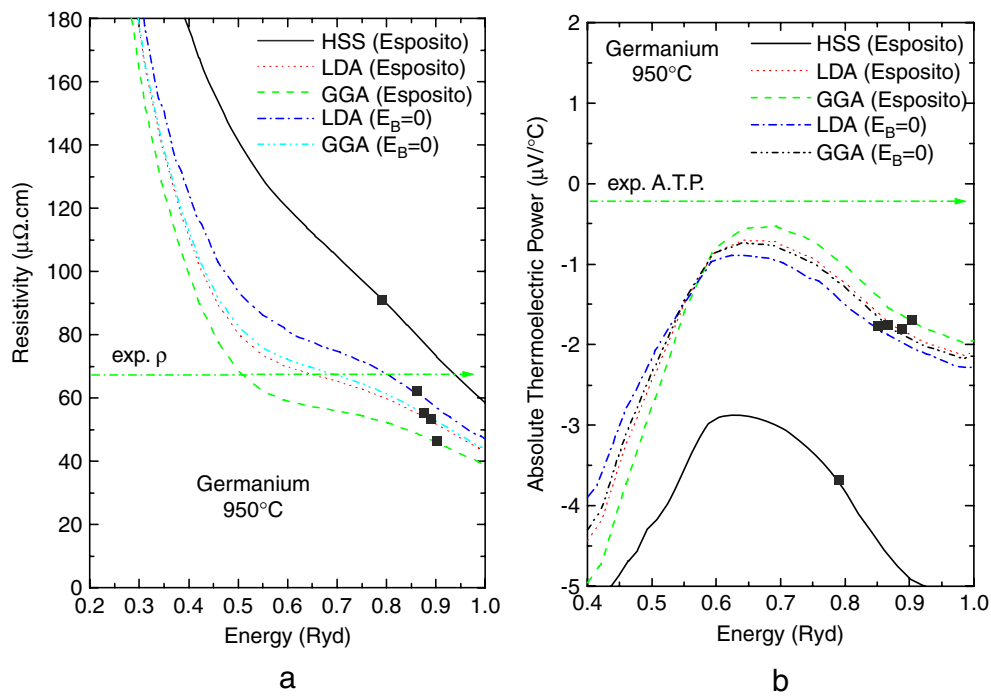


Figure 7. Why the ATP of normal metals is negative: example of germanium.

structure factor (figure 8). Indeed, the Fermi energy is situated near the maximum of the structure factor. If the Fermi energy is on the increasing side of the resistivity versus energy curve, the thermopower is positive. This is the case both for noble and for divalent metals. All our calculations (Makradi PhD thesis [15] (figures 9(a) and (b))) show clearly that the positive thermopower of zinc can be explained by the modulation of the 1/E curve by the peak of the structure factor. Noble metals also present a positive thermopower. The quantitative

calculations on liquid silver gives less accurate results due to the difficult problem of finding the Fermi energy if one takes into account the ten d electrons. The interesting result from a qualitative point of view is the apparition of a sharp resonance at the bottom of the s band (near 0.25 Ryd) due to the d density of states (figure 10(a)), giving a sharp resistivity peak. We only found a positive thermopower (figure 10(b)) by shifting the bottom of the conduction band E_B (unpublished results, Ben Hassine thesis [16]). This means that the 1/E resistivity

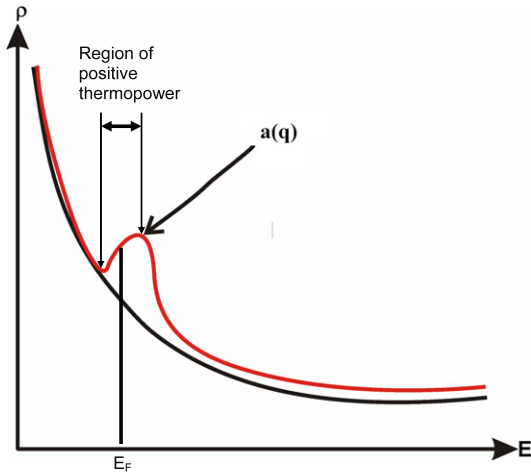


Figure 8. Modulation of the resistivity versus energy curve by the main peak of the structure factor and why the thermopower of noble and divalent metals is positive.

versus energy curve is also modulated by a sharp resonance scattering coming from the η_2 phase shift (figure 11(a)) [16]. This occurs for noble metals, but the Fermi energy lying in the structure factor modulation peak explains as for zinc the positive thermopower of silver. The resonance does not have a direct effect on the electronic transport properties. It is worth noticing that in certain circumstances (for example η_0 for Cd and Zn) we observed that a phase shift can cross the energy axis, inducing an anti-resonance traduced by a deep minimum in the resistivity versus energy curve. But we never observe that the three phase shifts cross the energy axis at the same energy, which would have given a funny ‘superconducting’ liquid metal resistivity strictly equal to zero.

4.3.3. Semi-metals with a gap or (and) pseudogap. Recently, we were interested in the thermopower of liquid antimony discussed in detail in another paper of this conference [17]. The thermopower of antimony is slightly positive and could not be explained by the position of the Fermi energy near the first peak of the structure factor nor by any d resonance (figure 12). So we searched and found another explanation. We must remember that the Ziman formula is only valid for a free electron band and that the density of states presents, according to Hafner [18], a gap that induces us to think that the valence has to be $Z = 3$. With $Z = 3$ we obtained a resistivity very near the experimental value (figure 12), but the thermopower is even more negative. So we have also to take into account the shape of the p density of states, which (as calculated by Hafner [18] and presented in his figure 7) is far from a free electron one. The DOS presents a sharp maximum, then a kind of pseudogap. So it is both necessary to take into account the existence of the gap and of a maximum in the p DOS followed by a pseudogap to understand the resistivity and ATP. We recalled that Mott *et al* [19] proposed to correct the mean free path at the Fermi energy by

$$L = L_{\text{Ziman}}/g^2 \quad \text{with } g = \left\{ \frac{n(E)}{n(E)_{\text{free}}} \right\}_{E_F} \quad (22)$$

and took the interatomic distance as the lowest value of the mean free path. Faber [20] demonstrated rigorously that

$$\rho = \frac{\rho_{\text{Ziman}}}{g^2}. \quad (23)$$

Consequently, one can correct the calculation of the resistivity at the Fermi energy. We pursued Faber’s calculation

$$\rho(E) = \frac{\rho_{\text{Ziman}}(E)}{g^2(E)} \quad (24)$$

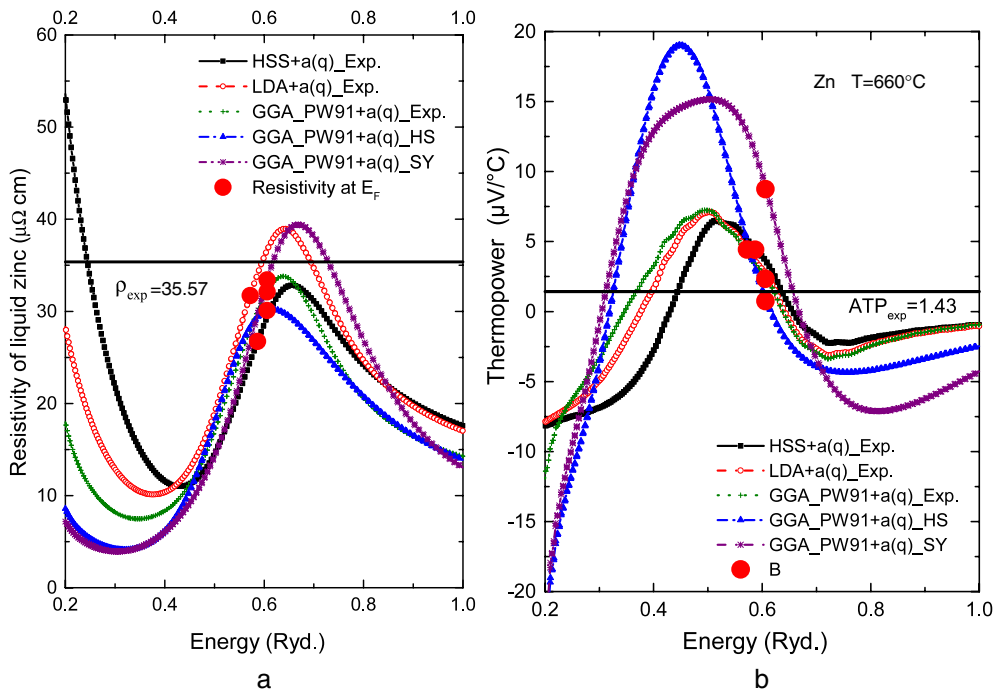


Figure 9. Explanation of the positive thermopower of liquid zinc.

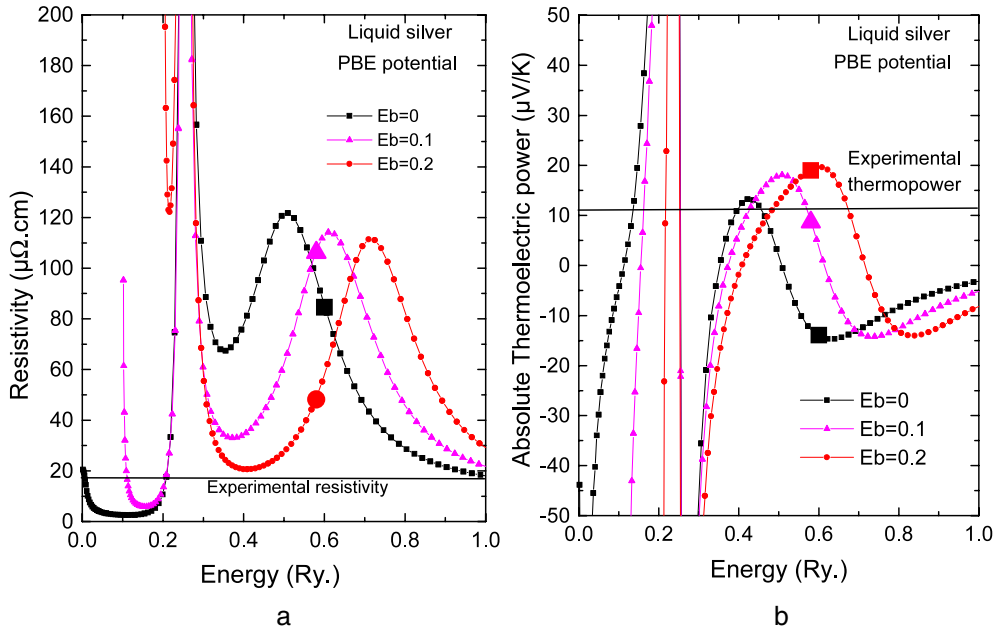


Figure 10. Explanation of the positive thermopower of liquid silver. Apparition of a resonance scattering at the bottom of the s band.

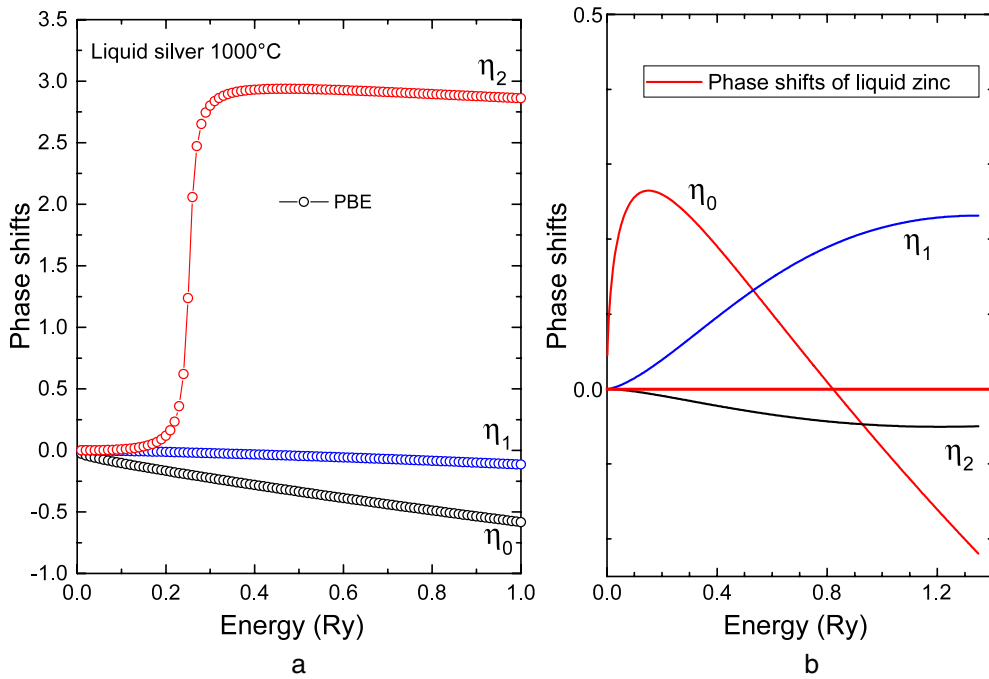


Figure 11. The resonance scattering of liquid silver is due to the fact that η_2 takes the value $\pi/2$. It also corresponds to a maximum in the density of states. In figure 11(b) one observes that the parameter η_0 passes through zero value, which corresponds to an anti-resonance.

by writing this equation at all energies and used the Hafner density of states to correct the resistivity by $g^2(E)$ in the whole domain of energy, then we differentiate it to obtain the thermopower. This may introduce a third modulation of the $1/E$ curve (figure 13).

In figure 14 we see clearly the effect of the pseudogap near 0.75 Ryd and the modulation by the $1/g^2$ curve. We also discovered that this modulation was not the reason of the positive thermopower of antimony, but that it comes from the fact that the true density of states is much greater than the free

electron one at the bottom of the p band, thus the Fermi energy is shifted from 0.56 Ryd to a much lower value (0.40 Ryd) and comes into the structure factor peak modulation.

4.3.4. Transition metals. For transition metals the Fermi energy is in the η_2 resonance peak, which is at the same energy as the structure factor modulation peak and is hidden by the resonance peak. This is illustrated in figure 15 (Zrouri *et al* [21]). However, the resonance peak induces a resistivity nearly five times greater than the experimental one. If one

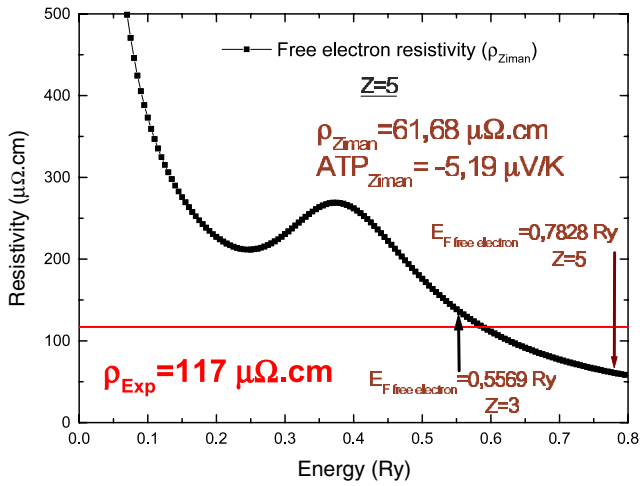


Figure 12. Resistivity versus energy for liquid antimony.

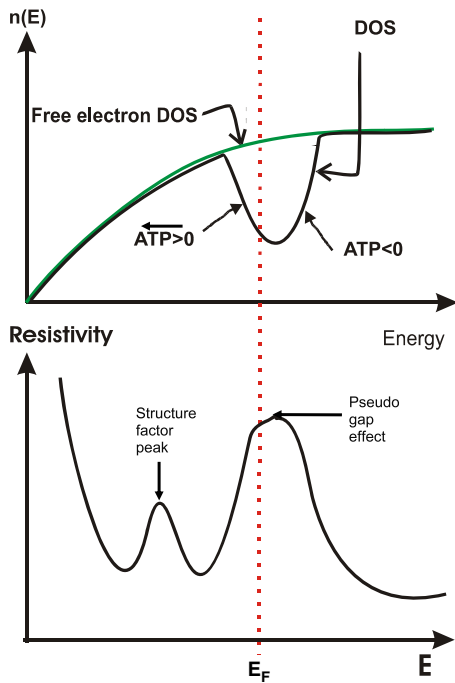


Figure 13. Schematic explanation of the modulation of the $1/E$ resistivity curve by a pseudogap.

examines the density of states obtained with the Lloyd formula, we observe that it is much higher and narrower than other DOS calculations, thus inducing a too sharp resistivity peak. It is thus necessary to improve the DOS calculation and thus the resistivity and thermopower. The solution was found in magnetic scattering effects; indeed, the electrons, either with spin up or down, ‘see’ a different manganese potential, since manganese presents a large number of unpaired electrons. Within our assumption, the potential felt by an electron of spin up differs from the one seen by an electron of spin down. This gives rise to a two-band conduction mechanism. The Ziman formula (19) written for the electron of spin α ($\alpha = \text{up or down}$) becomes

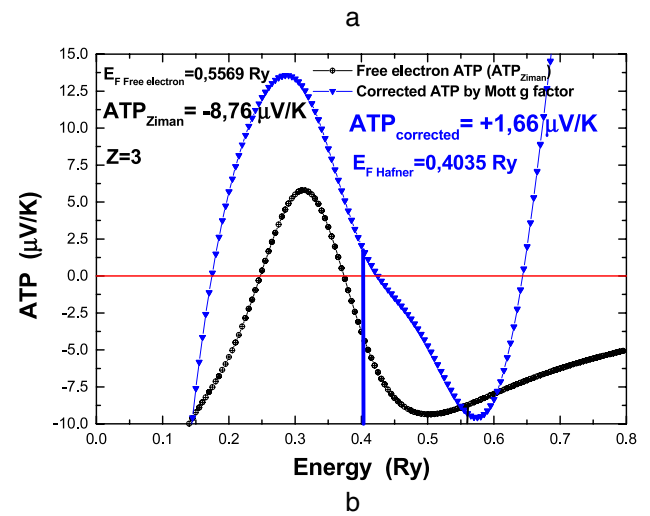
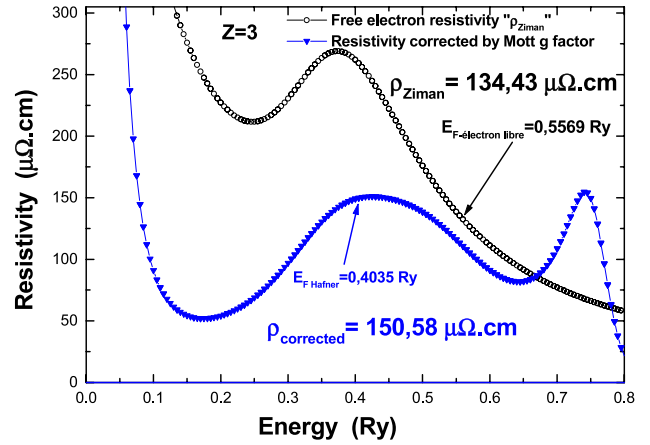


Figure 14. An explanation of the positive thermopower of antimony.

down) becomes

$$\rho^\alpha(E) = \frac{3\pi m_e^2 \Omega_0}{4e^2 \hbar^3 k^6} \int_0^{2k} a(q) |t^\alpha(q, E)|^2 q^3 dq \quad (25)$$

$$t^\alpha(q, E) = -\frac{2\pi \hbar^3}{m \sqrt{2mE\Omega_0}} \times \sum_l (2l+1) \sin \eta_l^\alpha(E) \cdot \exp(i\eta_l^\alpha(E)) P_l(\cos \theta). \quad (26)$$

The phase shifts $\eta^\alpha(E)$ are calculated from muffin tin potentials for each spin direction. The total resistivity is simply expressed as

$$\frac{1}{\rho} = \frac{1}{\rho^{\text{up}}} + \frac{1}{\rho^{\text{down}}}. \quad (27)$$

With this hypothesis we obtained a reasonable resistivity versus energy curve (figure 16). We can also deduce and explain why the first elements of the transition metal series like scandium have a positive thermopower while the last ones like nickel have a negative one.

4.3.5. *Liquid binary and ternary alloys.* In liquid alloys the Ziman formula is simply replaced by the Faber Ziman formula:

$$\rho_{\text{alloy}} = \frac{3\pi m^2}{\hbar^3 e^2 k_F^2} \Omega_0 \int_0^1 |t_{\text{alloy}}| ^2 4 \left(\frac{q}{2k_F} \right)^3 d \left(\frac{q}{2k_F} \right), \quad (28)$$

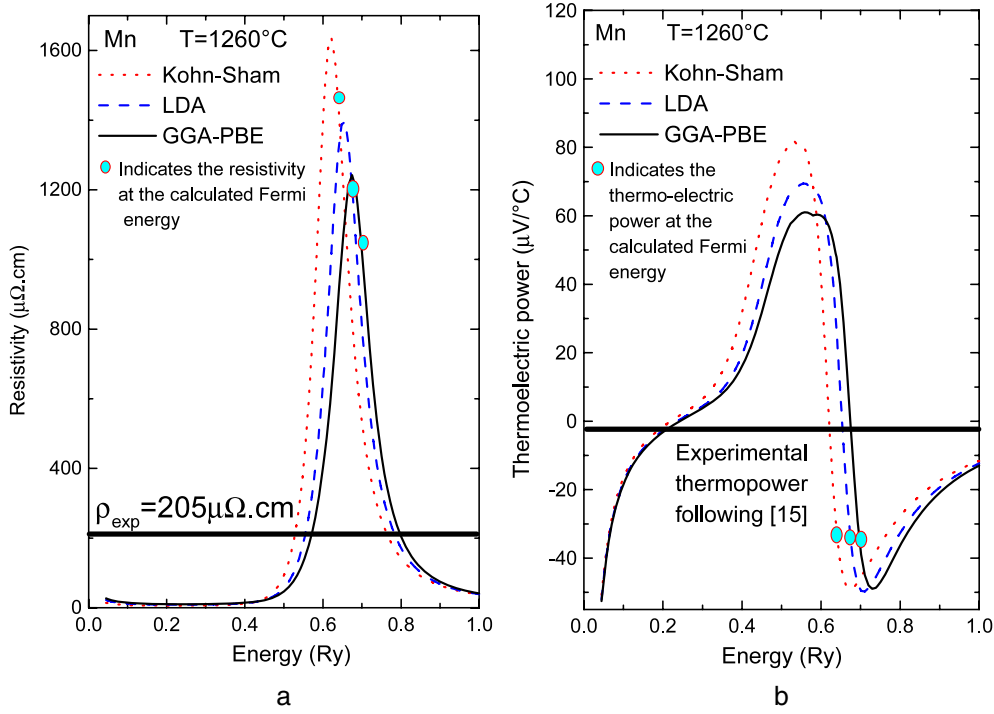


Figure 15. Spin independent calculation of the resistivity and thermopower of manganese.

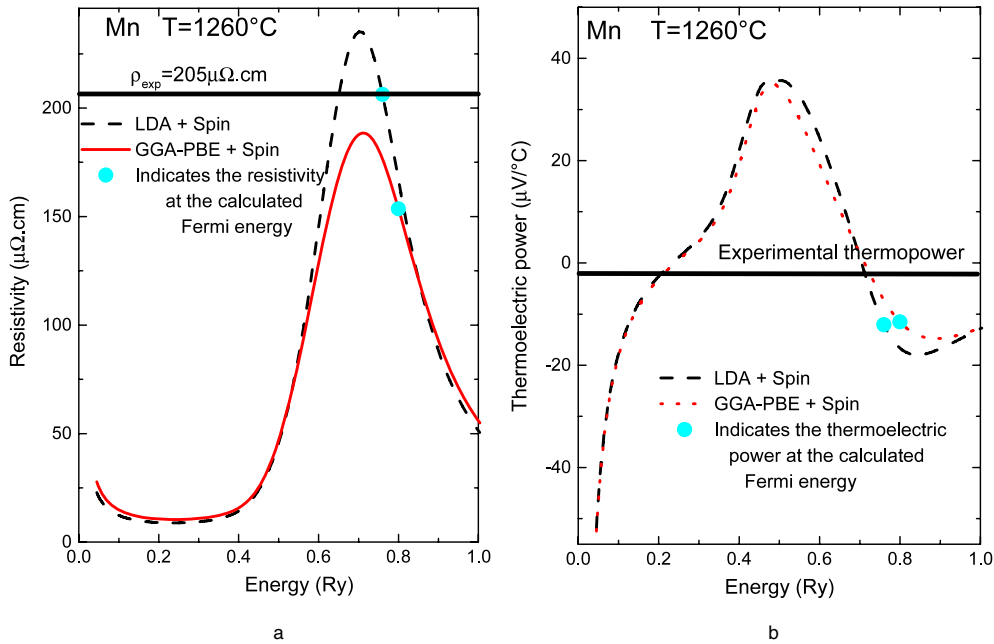


Figure 16. Spin dependent calculation of the resistivity and thermopower of manganese.

with

$$c_1 |t_1|^2 [1 - c_1 + c_1 a_{11}(q)] + c_2 |t_2|^2 [1 - c_2 + c_2 a_{22}(q)] + c_1 c_2 (t_1^* t_2 + t_1 t_2^*) [a_{12}(q) - 1], \quad (29)$$

where c_i are the concentrations, a_{ij} the partial structure factors and t_i the t matrix of element i in the alloy. In general, the resistivity and thermopower are nearly linear interpolations (or slightly convex) of the pure metals. However, in certain

circumstances it can happen that the Fermi energy, while changing the concentration, crosses a resonance peak, inducing larger resistivity or thermopower changes than expected by a more or less linear interpolation. An example can be given by the sodium–caesium alloy. The resistivity of caesium is about $80 \mu\Omega \text{ cm}$ while that of sodium is near $10 \mu\Omega \text{ cm}$. One expects a more or less linear decrease from 80 to $10 \mu\Omega \text{ cm}$. This is not the case, since the experimental resistivity increases

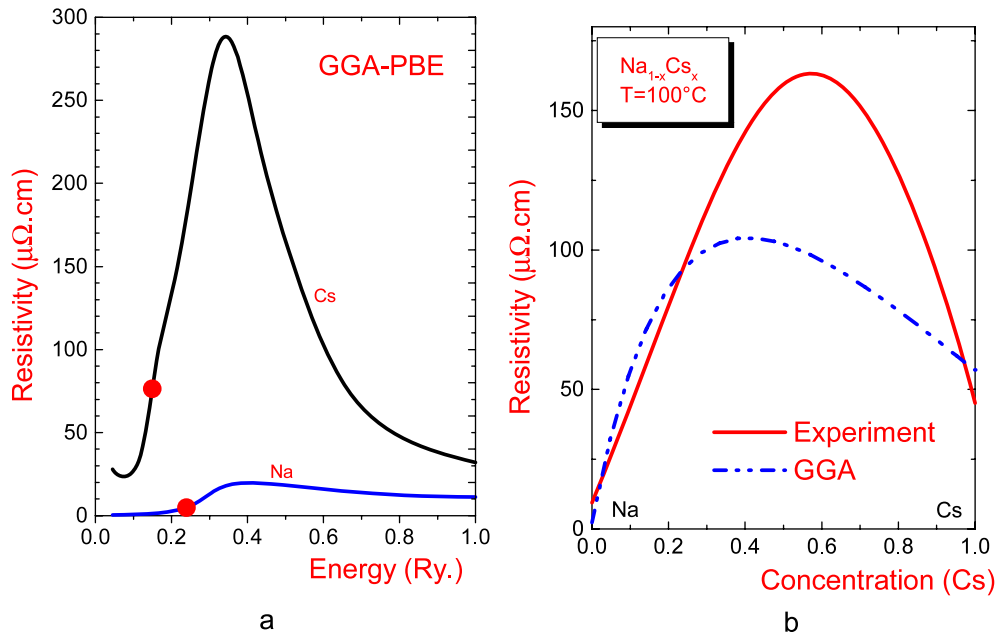


Figure 17. Resonant scattering for the Na–Cs alloy.

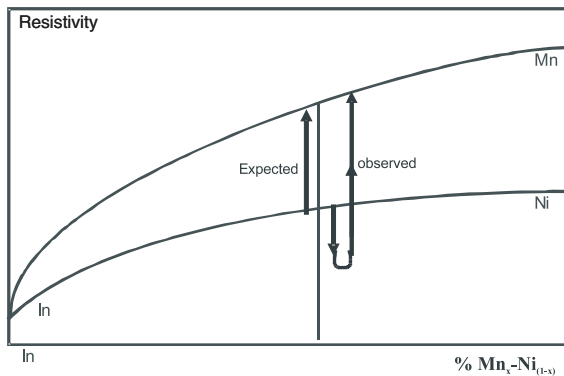


Figure 18. Schematic anomalous behaviour of the resistivity of ternary $\text{In}_{50}-(\text{Mn}_x-\text{Ni}_{(1-x)})_{50}$.

170 $\mu\Omega\text{ cm}$ in the middle of the phase diagram. If we plot the resistivity of caesium and sodium versus energy (figure 17) (Zroui’s thesis [22]), it shows clearly that adding sodium to caesium increases the Fermi energy, thus moves the resistivity of caesium into an η_2 resonance due to d electrons, and explains at least qualitatively the sharp increase. Similarly, some interesting results have been found and explained for Ni–Mn–In ternary alloys by Rhazi *et al* [23, 24]. Schematically, the resistivity of binary In–Ni and In–Mn is represented in figure 18. The resistivity increases from about 40 $\mu\Omega\text{ cm}$ for pure In to 80 $\mu\Omega\text{ cm}$ for pure Ni and 200 $\mu\Omega\text{ cm}$ for pure Mn. The aim of our study was to examine the Mn–Ni alloy. However, the measurement temperature being too high, we decreased it by adding indium as a third low temperature element. The resistivity became measurable. The contribution to the resistivity of indium is small. However, an important unexpected effect arises from the fact that indium, bringing free electrons, moved the Fermi energy in both

resonance peaks of manganese and nickel. We worked with 50 at.% In and substituted Mn with Ni. We expected to move regularly on the vertical line in the middle of the diagram of figure 18, increasing continuously from the resistivity of 50 at.% In–50 at.% Ni to 50 at.% In–50 at.% Mn. To our great surprise, adding manganese began to decrease the resistivity, which only increased above 50 at.% Mn (figure 19(a)). A possible qualitative explanation for this anomalous behaviour is proposed in figure 19(b). In this figure we have represented schematically the resistivity as a function of energy for pure Mn and Ni (without spin effects and with a crude exchange and correlation contribution). The resistivity of indium (not represented) is a gentle $1/E$ decreasing function of energy. Indium is a trivalent metal and brings three electrons per atom. We can understand the anomalous behaviour of the resistivity of the ternary alloy if we consider that if we replace Ni by Mn we move from the left to the right in the region of the full points (figure 19(b)). This means that the Fermi energy of Mn is higher than that of Ni. The resistivity is weighted by the concentration. With rich Ni content the resistivity begins to decrease (blue squares) when we increase the energy. But the weight of this curve becomes smaller when the concentration in manganese increases. Simultaneously, the weight of the manganese contribution increases (red circles). The thermopower of nickel rich alloys is negative (negative slope of the blue curve). As the concentration of manganese increases, the thermopower becomes less negative.

5. Conclusion

- (1) Different equations link the transport coefficients, especially the absolute thermoelectric power, the thermal and the electrical conductivities.

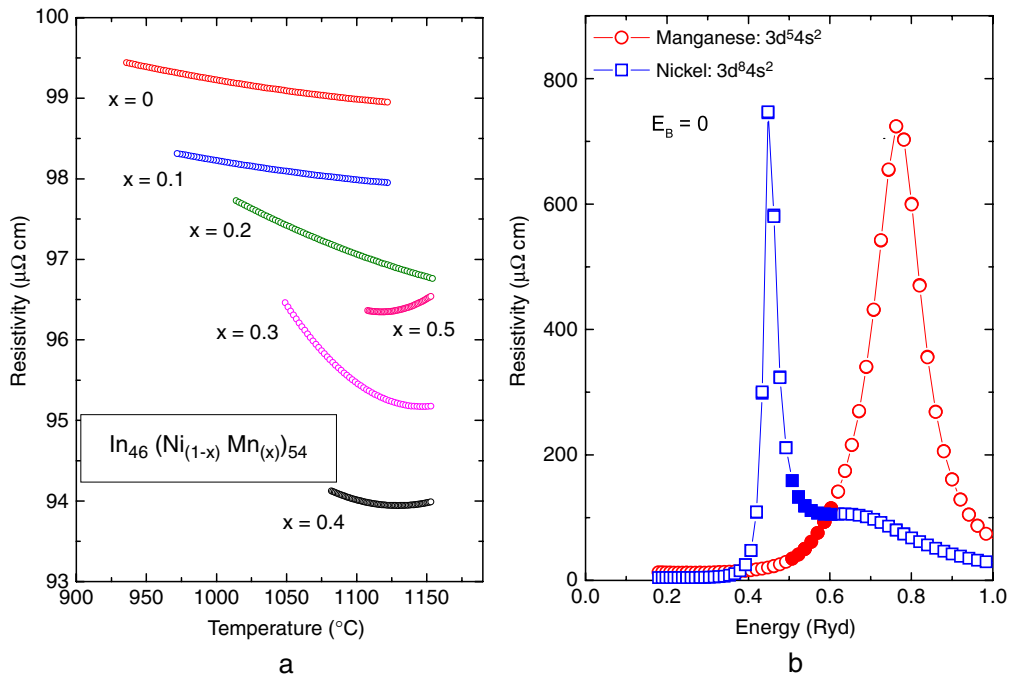


Figure 19. A tentative explanation of the resistivity of ternary $\text{In}_{50}-(\text{Mn}_x-\text{Ni}_{(1-x)})_{50}$.

- (2) The thermopower is proportional to the derivative of the resistivity with respect to energy. The resistivity versus energy is thus the key function.
- (3) The resistivity versus energy curve is a $1/E$ function modulated by
 - the structure factor,
 - the resonance of the squared t matrix,
 - the ratio of the density of states by the free electron one g .

The ATP is positive on the increasing side of each of these modulating functions.

The behaviour of alloys can also be understood in term of resistivity versus energy curves. The problem is to know how the Fermi energy shifts and passes through the modulation peaks. The contributions of the different metals are weighted by the composition, by the position of the peak of the structure factor and by the shift of the Fermi energy of the alloy in all these modulation peaks.

This formalism may explain the electronic transport properties of normal, noble, transition or semi-metals and alloys both in the liquid and in the amorphous state. It may also explain the metal–non-metal transition under the effect of high temperatures and pressures and the metal to non-metal transition when a pseudogap is created in semi-metals or bad semiconductors. The Ziman formula corrected by the g Mott factor is very interesting since it splits the Mott corrected Ziman formula into a scattering effect (mobility) and a number of conduction electrons linked to the true density of states at the Fermi energy.

6. Some open questions

It is worth asking if this new extended Ziman–Mott formula is not much more general than believed. In particular, can this formula be extended to solid polycrystalline materials and to high-temperature metals and alloys? The scattering is always described by a t matrix. Can the structure factor of a disordered liquid or amorphous metal be simply replaced by the structure factor of a real polycrystalline textured or not metallic alloy as schematically represented in figure 20(a)? Every experimentalist knows that adding only a few per cent of aluminium or of chromium to pure nickel gives either a positive or a negative ATP (in the chromel–alumel thermocouple). Can this be explained by a displacement of the Fermi energy through a structure peak of nickel identical to what happens in the liquid state when adding a second element? Is it possible to simply explain the nearly ten times smaller resistivity in solid metals by the Fermi energy being in the structure noise due to temperature, to impurities and to other defects? Is it possible to explain the high resistivity of a quasicrystal by the position of the Fermi energy being in a sharp diffraction peak (see for example figure 20(b) shown by Rapp [25] at the same conference)? Can this formula be adapted to (liquid) semiconductors by using the Kubo formula?

$$\sigma = - \int_{-\infty}^{+\infty} \sigma(E) \frac{\partial f(E)}{\partial E} dE. \quad (30)$$

Can two non-null contributions to the electronic transport where scattering of electrons may occur at E_V and E_C where $\sigma(E) = 1/\rho(E)$ be calculated with the Ziman–Mott formula? Can we consider that we may use

$$\sigma = \frac{1}{\rho(E_V)} + \frac{1}{\rho(E_C)}?$$

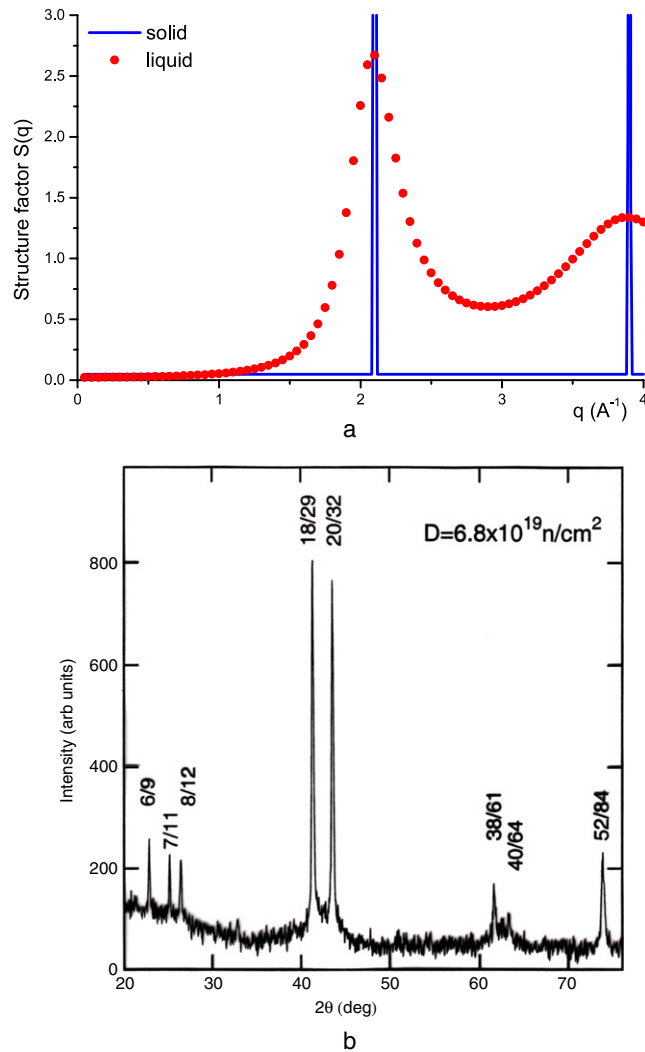


Figure 20. Can the Ziman–Mott formula explain the resistivity and thermopower of solid metals and alloys?

It is well known that the mobility of electrons is larger than that of ‘holes’. This is consistent with the fact that $\rho(E)$ is a nearly $1/E$ decreasing curve. This is also consistent with the sign of thermopower of semiconductors following the kind of dominant scatterers. Is this simply ‘by chance’?

Acknowledgments

The present work is a synthesis of my present reflexions on the electronic transport properties of liquid metals. This work would not have been possible without my collaboration with Professor Hugel to develop the potential and energy dependent phase shift calculations. The theoretical work has been developed by several students (Drs Makradi and Zrouri) in the frame of their PhDs, and later by Dr Ben Abdellah, also a PhD student and now assistant professor in a university in Morocco. Some of the present results have been included in the PhD thesis of some experimental PhD students (Drs Rhazi, Bestandji, Ben Hassine and Mhiaoui) who interpreted their measurements thanks to the programs elaborated. Thank you very much to all of them.

References

- [1] Smith A C, Janak J F and Adler R B 1967 *Electronic Conduction in Solids (Series in Phys. Quant. Electronics)* (New York: McGraw-Hill)
- [2] Barnard R D 1972 *Thermoelectricity in Metals and Alloys* (London: Taylor and Francis) p 30
- [3] Young W H 1985 *Electronic Transport Properties (Handbook of Thermodynamic and Transport Properties of Alkali Metals)* ed R W Ohse (Oxford: Blackwell Scientific Publications)
- [4] Giordanengo B, Benazzi N, Vinckel J, Gasser J G and Roubi L 1999 *J. Non-Cryst. Solids* **250–252** 377
- [5] Roberts R B, Righini F and Compton R C 1985 *Phil. Mag.* B **52** 114
- [6] Ziman J M 1966 *Phil. Mag.* **6** 1013
- [7] Faber T E and Ziman J M 1965 *Phil. Mag.* **11** 153
- [8] Evans R, Greenwood D A and Lloyd P 1971 *Phys. Lett. A* **35** 57
- [9] Dreirach O, Evans R, Güntherodt H J and Künzi U 1972 *J. Phys. F: Met. Phys.* **2** 709
- [10] Makradi A, Gasser J G, Hugel J, Yazı A and Bestandji M 1999 *J. Phys.: Condens. Matter* **11** 671
- [11] Mukhopadhyay G, Jain A and Ratti V K 1973 *Solid State Commun.* **13** 1623
- [12] Esposito E, Ehrenreich H and Gelatt C D 1978 *Phys. Rev. B* **18** 3913

- [13] Lloyd P 1967 *Proc. Phys. Soc.* **90** 207
- [14] Ben Abdellah A, Gasser J G, Makradi A, Grosdidier B and Hugel J 2003 *Phys. Rev. B* **68** 184201
- [15] Makradi A 1997 *Thèse de Doctorat* Université de Metz
- [16] Ben Hassine L 2000 *Thèse de Doctorat* Université de Metz
- [17] Mhiaoui S 2007 *Thèse de Doctorat* Université de Metz and this LAM13 conference
- [18] Hafner J and Jank W 1992 *Phys. Rev. B* **45** 2739–49
- [19] Mott N F and Davis E A 1971 *Electronic Processes in Non-crystalline Materials (International Series of Monographs on Physics)* (Oxford: Clarendon)
- [20] Faber T E 1972 *An Introduction to the Theory of Liquid Metals* (Cambridge: Cambridge University Press)
- [21] Zrouri H, Hugel J, Makradi A and Gasser J G 2001 *Phys. Rev. B* **64** 94202
- [22] Zrouri H 2001 *Thèse de Doctorat* Université de Metz
- [23] Rhazi A 1997 *Thèse de Doctorat* Université de Metz
- [24] Auchet J, Rhazi A and Gasser J G 1999 *J. Phys.: Condens. Matter* **11** 3043–50
- [25] Rapp O, Karkin A A, Goshchitskii B N, Voronin I, Srinivas V and Poon S J 2007 Electronic and atomic disorder in icosahedral AlPdRe *J. Phys.: Condens. Matter* **20** 114120